AIMS Mathematics, 10(1): 1757–1778.
DOI: 10.3934/math.2025080
Received: 28 October 2024
Revised: 05 January 2025
Accepted: 14 January 2025
Published: 24 January 2025

https://www.aimspress.com/journal/Math

Research article

Mixed finite element method for a time-fractional generalized Rosenau-RLW-Burgers equation

Ning Yang and Yang Liu*

School of Mathematical Sciences, Inner Mongolia University, Hohhot, 010021, China

* **Correspondence:** Email: mathliuyang@imu.edu.cn.

Abstract: In this article, the time-fractional generalized Rosenau-RLW-Burgers equation is numerically solved, where the generalized BDF2-θ is used to discretize the temporal direction, and the mixed finite element method is applied to the spatial direction. The stability of the fully discrete scheme is proven. Finally, the effectiveness of the numerical scheme is verified through some numerical examples, and the singularity of nonsmooth solutions in the initial time layer is effectively resolved by adding the correction term.

Keywords: time-fractional generalized Rosenau-RLW-Burgers equation; mixed finite element method; generalized BDF2-θ; stability; correction term; weak singularity
Mathematics Subject Classification: 24A33, 65M60, 65N30

1. Introduction

In this article, we consider the following time-fractional generalized Rosenau-RLW-Burgers equation:

$$u_t - {}_0^C D_t^\alpha u_{xx} + {}_0^C D_t^\beta u_{xxxx} + u_x - u_{xx} + f(u)_x = g(x,t),\ (x,t) \in \Omega \times J, \tag{1.1}$$

with boundary conditions

$$u(x,t) = u_{xx}(x,t) = 0,\ (x,t) \in \partial\Omega \times \bar{J}, \tag{1.2}$$

and initial condition

$$u(x,0) = u_0(x),\ x \in \Omega, \tag{1.3}$$

where $\Omega = (a,b)$ is the spatial domain, $J = (0,T]$ is the time interval with $T \in (0,\infty)$, and $g(x,t)$ is a known source term function. The nonlinear term $f(u)$ satisfies the assumption condition $|f(u)| \le c_f(u)|u|$, where $c_f(u)$ is a positive constant on u. ${}_0^C D_t^\alpha u$ and ${}_0^C D_t^\beta u$ are both Caputo fractional derivatives with $0 < \alpha, \beta < 1$. Since ${}_0^C D_t^\gamma u = \frac{\partial^\gamma (u-u_0)}{\partial t^\gamma}$, all of the above Caputo fractional derivatives can be converted

into the Riemann-Liouville fractional derivative, note that

$$\frac{\partial^\gamma u}{\partial t^\gamma} = \frac{1}{\Gamma(1-\gamma)}\frac{\partial}{\partial t}\int_0^t \frac{u(x,s)}{(t-s)^\gamma}\mathrm{d}s,\ 0<\gamma<1. \tag{1.4}$$

Specifically, when $\alpha = 1$, $\beta = 1$, (1.1) degenerates into the generalized Rosenau-RLW-Burgers equation which can be seen as the combined system between the generalized Rosenau-RLW equation and the generalized Rosenau-Burgers equation.

The RLW equation, the Rosenau equation, and their combined systems with other equations are significant mathematical and physical equations that effectively describe nonlinear wave behaviors. These equations have become interesting topics in the study of nonlinear dispersion dynamics. Since obtaining analytical solutions for these equations is challenging, studying their numerical methods is paramount. Over the years, there has been extensive research on numerical methods for solving this type of equation. In [1], Atouani and Omrani discussed the numerical solution of the Rosenau-RLW (RRLW) equation based on the Galerkin finite element method. In [2], He and Pan developed a three-level, linearly implicit finite difference method for solving the generalized Rosenau-Kawahara-RLW equation. In [3], Wongsaijai and Poochinapan developed a pseudo-compact finite difference scheme for solving the generalized Rosenau-RLW-Burgers equation. In [4], Mouktonglang et al. analyzed a generalized Rosenau-RLW-Burgers equation with periodic initial-boundary value. For more papers on related equations, please refer to [5–8]. It is worth noting that the literature on the fractional generalized Rosenau-RLW-Burgers equation is relatively scarce, and its analytical solution is difficult to obtain. Therefore, we have to consider effective numerical methods such as finite element methods [9–12], finite difference methods [13–15], finite volume methods [16], spectral methods [17–19], and mixed finite element methods [20–22]. In addition, the existence of time-fractional derivatives increases the difficulty of studying numerical methods. Therefore, it is crucial to choose an appropriate high-order approximation formula for the fractional derivative to establish a stable numerical scheme for (1.1).

In 1986, Lubich [23] proposed the convolution quadrature (CQ) formula for Riemann Liouville fractional operators using the discrete convolution. In [24], Chen et al. developed an alternating direction implicit fractional trapezoidal rule type to solve a two-dimensional fractional evolution equation. In [25], Jin et al. proposed a corrected approximation formula for high-order BDFs through appropriate initial modifications to discretize fractional evolution equations. Based on the CQ formula, in [26], Liu et al. developed the shifted convolution quadrature (SCQ) theory, which extended the CQ formula at $x_{n-\theta}$ and discussed the constraints of parameter θ. In [27], Yin et al. studied the generalized BDF2-θ with the finite element method for solving the fractional mobile/immobile transport model, and also developed a correction scheme by adding the starting part to restore convergence order. For more related papers, please refer to [28–33].

In this article, we develop the generalized BDF2-θ in time combined with the mixed finite element method in space to solve (1.1). The focuses of this article are as follows:

- It is noted that the time-fractional generalized Rosenau-RLW-Burgers equation containing two time-fractional operators is studied.
- The stability of the time-fractional generalized Rosenau-RLW-Burgers equation (1.1) based on the mixed finite element method is given.
- Based on a comprehensive analysis of some numerical examples, the numerical method's

feasibility and effectiveness have been extensively validated. Specifically, the issue of decreasing the convergence rate of nonsmooth solutions is solved by adding correction terms.

The structure of this article is as follows: In Section 2, the generalized BDF2-θ is introduced, and the fully discrete mixed finite element scheme is provided. In Section 3, the existence and uniqueness theorem for the fully discrete mixed finite element scheme is given. In Section 4, the stability of the scheme is proved. In Section 5, some numerical examples with smooth and nonsmooth solutions based on the discrete scheme are presented. In Section 6, some conclusions are given.

2. Numerical scheme

In this section, we present the fully discrete mixed finite element scheme for (1.1) in space, which combines the generalized BDF2-θ in time. The generalized BDF2-θ with the starting part is introduced in [27]. Further, we divide the time interval $[0, T]$ into $0 = t_0 < t_1 < \cdots < t_{N-1} < t_N = T$, and let $t_n = n\tau$ $(n = 1, 2, \cdots, N)$, where τ is time step length size and N is a positive integer.

For the convenience of research, set $\hat{u} := u - u_0$, and assume that $\hat{u}$ has the following form:

$$\hat{u}(x,t) = \hat{u}_1(x,t) + \hat{u}_2(x,t) := \sum_{j=1}^{\kappa} c_j t^{\sigma_j} + t^{\sigma_{\kappa+1}}\phi(x,t), \tag{2.1}$$

where $c_j = c(x)$, $1 < \sigma_1 < \sigma_2 < \cdots < \sigma_\kappa < \sigma_{\kappa+1}$ and $\phi(x,t)$ is sufficiently differentiable with respect to t.

Using $\hat{u} := u - u_0$, we can write (1.1)–(1.3) as

$$\hat{u}_t - \frac{\partial^\alpha \hat{u}_{xx}}{\partial t^\alpha} + \frac{\partial^\beta \hat{u}_{xxxx}}{\partial t^\beta} + \hat{u}_x - \hat{u}_{xx} + f(\hat{u})_x = \hat{g}(x,t),\ (x,t) \in \Omega \times J, \tag{2.2}$$

with boundary conditions

$$\hat{u}(x,t) = \hat{u}_{xx}(x,t) = 0,\ (x,t) \in \partial\Omega \times \bar{J}, \tag{2.3}$$

and initial condition

$$\hat{u}(x,0) = 0,\ x \in \Omega, \tag{2.4}$$

where $\hat{g}(x,t) = g(x,t) + (u_0)_x - (u_0)_{xx}$.

Now, we introduce an auxiliary variable $q = \hat{u}_{xx}$ to obtain the following coupled system:

$$\hat{u}_t - \frac{\partial^\alpha \hat{u}_{xx}}{\partial t^\alpha} + \frac{\partial^\beta q_{xx}}{\partial t^\beta} + \hat{u}_x - \hat{u}_{xx} + f(\hat{u})_x = \hat{g}(x,t), \tag{2.5}$$

and

$$q = \hat{u}_{xx}. \tag{2.6}$$

Multiplying (2.5) and (2.6) by $v \in H_0^1$ and $w \in H_0^1$, respectively, integrating the result equations, and using integration by parts, we obtain the following weak form:

$$(\hat{u}_t, v) + (\frac{\partial^\alpha \hat{u}_x}{\partial t^\alpha}, v_x) - (\frac{\partial^\beta q_x}{\partial t^\beta}, v_x) - (\hat{u}, v_x) + (\hat{u}_x, v_x) - (f(\hat{u}), v_x) = (\hat{g}, v),\ \forall v \in H_0^1, \tag{2.7}$$

and

$$(q, w) + (\hat{u}_x, w_x) = 0,\ \forall w \in H_0^1. \tag{2.8}$$

To provide the fully discrete numerical scheme, we first introduce the relevant formulas and lemmas for the generalized BDF2-θ.

For smooth functions $\hat{u}$ and q in $[0, T]$, we let $\hat{u}^n = \hat{u}(\cdot, t_n)$, $q^n = (\cdot, t_n)$. The approximation formula for the Riemann-Liouville fractional derivative at time $t_{n-\theta}$ with the generalized BDF2-θ is

$$\begin{aligned}\frac{\partial^\gamma \hat{u}^{n-\theta}}{\partial t^\gamma} &= \tau^{-\gamma}\sum_{j=0}^{n}\omega_j^{(\gamma)}\hat{u}^{n-j} + \tau^{-\gamma}\sum_{j=1}^{\kappa}\omega_{n,j}^{(\gamma)}\hat{u}^j + R_\gamma^{n-\theta}\\ &:= \Psi_\tau^{\gamma,n}\hat{u} + S_{\tau,\kappa}^{\gamma,n}\hat{u} + R_\gamma^{n-\theta},\end{aligned} \tag{2.9}$$

where $|R_\gamma^{n-\theta}| \le C\tau^2$.

The discrete convolution part is denoted as

$$\Psi_\tau^{\gamma,n}\hat{u} := \tau^{-\gamma}\sum_{j=0}^{n}\omega_j^{(\gamma)}\hat{u}^{n-j}, \tag{2.10}$$

and the starting part is

$$S_{\tau,\kappa}^{\gamma,n}\hat{u} := \tau^{-\gamma}\sum_{j=1}^{\kappa}\omega_{n,j}^{(\gamma)}\hat{u}^j. \tag{2.11}$$

The convolution weights $\{\omega_j^{(\gamma)}\}_{j=0}^{\infty}$ in (2.10) are generated by the following generating function:

$$\omega^{(\gamma)}(\xi) = \left(\frac{3\gamma-2\theta}{2\gamma} - \frac{2\gamma-2\theta}{\gamma}\xi + \frac{\gamma-2\theta}{2\gamma}\xi^2\right)^\gamma. \tag{2.12}$$

Lemma 2.1. *[27] We give the convolution weights $\{\omega_j^{(\gamma)}\}_{j=0}^{\infty}$ of the generalized BDF2-θ as follows:*

$$\begin{aligned}&\omega_0^{(\gamma)} = \left(\frac{3\gamma-2\theta}{2\gamma}\right)^\gamma, \quad \omega_1^{(\gamma)} = 2(\theta-\gamma)\left(\frac{2\gamma}{3\gamma-2\theta}\right)^{1-\gamma},\\ &\omega_j^{(\gamma)} = \frac{2\gamma}{j(3\gamma-2\theta)}\left[2(\gamma-\theta)\left(\frac{j-1}{\gamma}-1\right)\omega_{j-1}^{(\gamma)} + (\gamma-2\theta)\left(1-\frac{j-2}{2\gamma}\right)\omega_{j-2}^{(\gamma)}\right], \quad j \ge 2.\end{aligned} \tag{2.13}$$

Lemma 2.2. *[27] The starting weights $\{\omega_{n,j}^{(\gamma)}\}_{j=1}^{\kappa}$ of the generalized BDF2-θ are given as the following:*

$$\sum_{j=1}^{\kappa}\omega_{n,j}^{(\gamma)}j^\ell = \frac{\Gamma(\ell+1)}{\Gamma(\ell-\gamma+1)}(n-\theta)^{\ell-\gamma} - \sum_{j=1}^{n}\omega_{n-j}^{(\gamma)}j^\ell, \quad \ell = \sigma_1, \sigma_2, \cdots, \sigma_\kappa. \tag{2.14}$$

Lemma 2.3. *[12, 15] For $\hat{u} \in C^4[0,\pi]$, the following two approximate formulas at $t_{n-\theta}$ hold:*

$$\begin{aligned}g(t_{n-\theta}) &= g^{n-\theta} + O(\tau^2),\\ f(\hat{u}(t_{n-\theta})) &= f(\hat{u}^{n-\theta}) + O(\tau^2),\end{aligned} \tag{2.15}$$

where $g^{n-\theta} := (1-\theta)g^n + \theta g^{n-1}$ and $f(\hat{u}^{n-\theta}) := (2-\theta)f(\hat{u}^{n-1}) - (1-\theta)f(\hat{u}^{n-2})$.

Next, we have the following approximate formula:

$$\begin{aligned}\hat{u}(t_{n-\theta}) &= \hat{u}^{n-\theta} + S^{0,n}_{\tau,\kappa}\hat{u} + O(\tau^2)\\ &:= (1-\theta)\hat{u}^n + \theta\hat{u}^{n-1} + S^{0,n}_{\tau,\kappa}\hat{u} + O(\tau^2).\end{aligned} \tag{2.16}$$

Without considering the starting part, we can obtain the weak form of (2.5) and (2.6) at $t_{n-\theta}$:

$$\begin{aligned}&(\Psi^{1,n}_{\tau}\hat{u}, v) + (\Psi^{\alpha,n}_{\tau}\hat{u}_x, v_x) - (\Psi^{\beta,n}_{\tau}q_x, v_x) - (\hat{u}^{n-\theta}, v_x) + (\hat{u}^{n-\theta}_x, v_x)\\ =&(f(\hat{u}^{n-\theta}), v_x) + (\hat{g}^{n-\theta}, v) - (R^{n-\theta}_1, v),\end{aligned} \tag{2.17}$$

and

$$(q^{n-\theta}, w) + (\hat{u}^{n-\theta}_x, w_x) = -(R^{n-\theta}_2, w), \tag{2.18}$$

where $R^{n-\theta}_1 = O(\tau^2)$ and $R^{n-\theta}_2 = O(\tau^2)$.

To establish the fully discrete mixed finite element scheme, we introduce the following finite element space:

$$V_h = \{v_h | v_h \in H^1_0, v_h|_{I_i} \in P_k(I_i),\ \forall I_i \in \mathcal{T}_h, k \geq 1\},$$

where $\mathcal{T}_h$ is a subdivision of $\bar{\Omega} = [a, b]$ into M subintervals $I_i = [x_{i-1}, x_i]$, with $h_i = x_i - x_{i-1}$, $h = \max\limits_{1\leq i\leq M} h_i$, and $P_k(I_i)$ represent the polynomials with a degree less than or equal to k in I_i.

Next, we provide linear basis functions $\{\varphi_i\}^M_{i=1}$ of finite element space V_h as follows:

$$\varphi_i(x) = \begin{cases} 1 + \frac{x-x_i}{h_i}, & x \in I_i,\\ 1 - \frac{x-x_i}{h_{i+1}}, & x \in I_{i+1},\\ 0, & \text{others},\end{cases} \tag{2.19}$$

$$\varphi_M(x) = \begin{cases} 1 + \frac{x-x_M}{h_M}, & x \in I_M,\\ 0, & \text{others}.\end{cases} \tag{2.20}$$

Based on the above finite element space, we find $\{U^{n-\theta}, Q^{n-\theta}\} \in V_h \times V_h$ satisfying

$$\begin{aligned}&(\Psi^{1,n}_{\tau}U, V) + (\Psi^{\alpha,n}_{\tau}U_x, V_x) - (\Psi^{\beta,n}_{\tau}Q_x, V_x) - (U^{n-\theta}, V_x) + (U^{n-\theta}_x, V_x)\\ =&(f(U^{n-\theta}), V_x) + (\hat{g}^{n-\theta}, V),\ \forall V \in V_h,\end{aligned} \tag{2.21}$$

and

$$(Q^{n-\theta}, W) + (U^{n-\theta}_x, W_x) = 0,\ \forall W \in V_h. \tag{2.22}$$

3. Existence and uniqueness of numerical solution

Theorem 3.1. *The solution of the fully discrete mixed finite element scheme* (2.21) *and* (2.22) *is uniquely solvable.*

Proof. Taking basis functions $\{\varphi_i\}^M_{i=1}$ of finite element space V_h, we have

$$U^n = \sum_{i=1}^{M} u^n_i\varphi_i, \quad Q^n = \sum_{i=1}^{M} q^n_i\varphi_i. \tag{3.1}$$

Taking $V = \varphi_j$ and $W = \varphi_j$ from (2.21) and (2.22), we have

$$\begin{aligned}&\tau^{-1}\omega_0^{(1)}A\mathbf{U^n} + \tau^{-\alpha}\omega_0^{(\alpha)}B\mathbf{U^n} + (1-\theta)B\mathbf{U^n} - (1-\theta)C\mathbf{U^n} - \tau^{-\beta}\omega_0^{(\beta)}B\mathbf{Q^n}\\ =&\mathbf{F}^{n-\theta} + \mathbf{G}^{n-\theta} - \tau^{-1}\sum_{k=1}^{n}\omega_k^{(1)}A\mathbf{U^{n-k}} - \tau^{-\alpha}\sum_{k=1}^{n}\omega_k^{(\alpha)}B\mathbf{U^{n-k}}\\ &- \theta B\mathbf{U^{n-1}} + \theta C\mathbf{U^{n-1}} + \tau^{-\beta}\sum_{k=1}^{n}\omega_k^{(\beta)}B\mathbf{Q^{n-k}},\end{aligned} \tag{3.2}$$

and

$$(1-\theta)B\mathbf{U^n} + (1-\theta)A\mathbf{Q^n} = -\theta B\mathbf{U^n} - \theta A\mathbf{Q^n}, \tag{3.3}$$

where

$$\begin{aligned}&A = \left[(\varphi_i,\varphi_j)\right]_{1\le i,j\le M}^T,\ B = \left[(\varphi_{ix},\varphi_{jx})\right]_{1\le i,j\le M}^T,\ C = \left[(\varphi_i,\varphi_{jx})\right]_{1\le i,j\le M}^T,\\ &\mathbf{F^{n-\theta}} = \left[\left(f(U^{n-\theta}),\varphi_{1x}\right),\cdots,\left(f(U^{n-\theta}),\varphi_{Mx}\right)\right]^T,\ \mathbf{G^{n-\theta}} = \left[\left(g^{n-\theta},\varphi_1\right),\cdots,\left(g^{n-\theta},\varphi_M\right)\right]^T.\end{aligned}$$

Obviously, A and B are symmetric and positive definite. Further, processing the boundary and simplifying the right-hand term, we have

$$\left(\tau^{-1}\omega_0^{(1)}\widetilde{A} + \tau^{-\alpha}\omega_0^{(\alpha)}\widetilde{B} + (1-\theta)\widetilde{B} - (1-\theta)\widetilde{C}\right)\mathbf{U}^n - \tau^{-\beta}\omega_0^{(\beta)}\widetilde{B}\mathbf{Q}^n = \mathbf{H}_1^n, \tag{3.4}$$

and

$$(1-\theta)\widetilde{B}\mathbf{U}^n + (1-\theta)\widetilde{A}\mathbf{Q}^n = \mathbf{H}_2^n, \tag{3.5}$$

where

$$\begin{aligned}\mathbf{H}_1^n =&\mathbf{F}^{n-\theta} + \mathbf{G}^{n-\theta} - \tau^{-1}\sum_{k=1}^{n}\omega_k^{(1)}A\mathbf{U^{n-k}} - \tau^{-\alpha}\sum_{k=1}^{n}\omega_k^{(\alpha)}B\mathbf{U^{n-k}} - \theta B\mathbf{U^{n-1}}\\ &+ \theta C\mathbf{U^{n-1}} + \tau^{-\beta}\sum_{k=1}^{n}\omega_k^{(\beta)}B\mathbf{Q^{n-k}},\\ \mathbf{H}_2^n =& -\theta B\mathbf{U^n} - \theta A\mathbf{Q^n}.\end{aligned}$$

Multiplying (3.4) by $\tau\widetilde{A}^{-1}$, we have

$$\left(\omega_0^{(1)}E + \tau^{1-\alpha}\omega_0^{(\alpha)}\widetilde{A}^{-1}\widetilde{B} + \tau(1-\theta)\widetilde{A}^{-1}\widetilde{B} - \tau(1-\theta)\widetilde{A}^{-1}\widetilde{C}\right)\mathbf{U}^n - \tau^{1-\beta}\omega_0^{(\beta)}\widetilde{A}^{-1}\widetilde{B}\mathbf{Q}^n = \tau\widetilde{A}^{-1}\mathbf{H}_1^n. \tag{3.6}$$

Further, rewrite (3.5) as

$$\mathbf{Q}^n = \mathbf{H}_3^n, \tag{3.7}$$

where $\mathbf{H}_3^n = (1-\theta)^{-1}\widetilde{A}^{-1}\mathbf{H}_2^n - \widetilde{A}^{-1}\widetilde{B}\mathbf{U}^n$.

Substitute (3.7) into (3.6) to obtain

$$\mathbf{K}\mathbf{U}^n = \mathbf{H}_4^n, \tag{3.8}$$

where

$$\mathbf{K} = \omega_0^{(1)} E + \tau^{1-\alpha}\omega_0^{(\alpha)}\widetilde{A}^{-1}\widetilde{B} + \tau(1-\theta)\widetilde{A}^{-1}\widetilde{B} - \tau(1-\theta)\widetilde{A}^{-1}\widetilde{C} + \tau^{1-\beta}\omega_0^{(\beta)}\widetilde{A}^{-1}\widetilde{B}\widetilde{A}^{-1}\widetilde{B},$$

$$\mathbf{H}_4^n = \tau\widetilde{A}^{-1}\mathbf{H}_1^n + \tau^{1-\beta}(1-\theta)^{-1}\omega_0^{(\beta)}\widetilde{A}^{-1}\widetilde{B}\widetilde{A}^{-1}\mathbf{H}_2^n.$$

It is easy to see that (3.7) and (3.8) are equivalent to (3.4) and (3.5). Due to τ being small enough and E being an identity matrix, the matrix $\mathbf{K}$ is invertible. Additionally, since U^k $(k = 0, 1, \cdots, n-1)$ is known, after multiple iterations, (3.7) and (3.8) have a unique solution. □

Remark 3.1. *Since we introduce the auxiliary variable $q = \hat{u}_{xx}$ to transform* (2.2) *into a first-order system* (2.5) *and* (2.6)*, according to [34, 35], the mixed finite element scheme* (2.21) *and* (2.22) *do not need to satisfy the LBB condition. In [36], the LBB condition is a condition for the problem to be well posed. From this perspective, typically satisfying the LBB condition is to obtain the existence and uniqueness of a solution. Although the mixed finite element scheme in this article does not need to satisfy the LBB condition, it still satisfies the existence and uniqueness of a solution.*

4. Stability

Lemma 4.1. *[12, 14] For $\forall U^m \in V_h$, satisfying $U^m = 0$ $(m < 0)$, we have*

$$(\Psi_t^{1,m} U, U^{m-\theta}) \geq \frac{1}{4\tau}(\mathbb{H}[U^m] - \mathbb{H}[U^{m-1}]),\ m \geq 1,$$

where

$$\mathbb{H}[U^m] = (3-2\theta)\|U^m\|^2 - (1-2\theta)\|U^{m-1}\|^2 + (2-\theta)(1-2\theta)\|U^m - U^{m-1}\|^2,$$

and

$$\mathbb{H}[U^m] \geq \frac{1}{1-\theta}\|U^m\|^2,\ m \geq 1.$$

Lemma 4.2. *[27] For any vector $(v^0, v^1, \cdots, v^{n-1}) \in \mathbb{R}^n$, defining $\{\omega_k^{(\gamma)}\}_{k=0}^{\infty}$ $(0 < \gamma < 1)$ be a sequence of coefficients of the generating function $\omega^{(\gamma)}(\xi)$ in (2.12) and $0 \leq \theta \leq \min\{\gamma, \frac{1}{2}\}$, we have*

$$\sum_{m=1}^{n-1} v^m \sum_{k=1}^{m} \omega_{m-k}^{(\gamma)} v^k \geq 0,\ n \geq 1.$$

Theorem 4.1. *Let $u_h^n = U^n + \bar{u}_h^0$, where $\bar{u}_h^0$ is an approximation of u_0, the following stability of the fully discrete scheme (2.21) and (2.22) holds:*

$$\|u_h^L\|^2 \ \leq\ C\left(\|\bar{u}_h^0\|^2 + \tau\sum_{n=1}^{L}\|g^{n-\theta}\|^2\right),\ 1 \leq L \leq N, \tag{4.1}$$

where C is a positive constant independent of h and τ.

Proof. Taking $V = U^{n-\theta}$, $W = \Psi_\tau^{\beta,n} Q$, (2.21) and (2.22) can be written as

$$\begin{aligned}&(\Psi_\tau^{1,n} U, U^{n-\theta}) + (\Psi_\tau^{\alpha,n} U_x, U_x^{n-\theta}) - (\Psi_\tau^{\beta,n} Q_x, U_x^{n-\theta}) + \|U_x^{n-\theta}\|^2\\ =&(U^{n-\theta}, U_x^{n-\theta}) + (f(U^{n-\theta}), U_x^{n-\theta}) + (\hat{g}^{n-\theta}, U^{n-\theta}),\end{aligned} \tag{4.2}$$

and

$$(Q^{n-\theta}, \Psi_\tau^{\beta,n} Q) + (U_x^{n-\theta}, \Psi_\tau^{\beta,n} Q_x) = 0. \tag{4.3}$$

Adding (4.2) and (4.3), we have

$$\begin{aligned} &(\Psi_\tau^{1,n} U, U^{n-\theta}) + (\Psi_\tau^{\alpha,n} U_x, U_x^{n-\theta}) + (Q^{n-\theta}, \Psi_\tau^{\beta,n} Q) + \|U_x^{n-\theta}\|^2 \\ =&(U^{n-\theta}, U_x^{n-\theta}) + (f(U^{n-\theta}), U_x^{n-\theta}) + (\hat{g}^{n-\theta}, U^{n-\theta}). \end{aligned} \tag{4.4}$$

Using Lemma 4.1, we obtain

$$\begin{aligned} &\frac{1}{4\tau}(\mathbb{H}[U^n] - \mathbb{H}[U^{n-1}]) + (\Psi_\tau^{\alpha,n} U_x, U_x^{n-\theta}) + (Q^{n-\theta}, \Psi_\tau^{\beta,n} Q) + \|U_x^{n-\theta}\|^2 \\ \le&(U^{n-\theta}, U_x^{n-\theta}) + (f(U^{n-\theta}), U_x^{n-\theta}) + (\hat{g}^{n-\theta}, U^{n-\theta}). \end{aligned} \tag{4.5}$$

Multiply (4.5) by 4τ and sum it with respect to n from 1 to L to get

$$\begin{aligned} &\mathbb{H}[U^L] - \mathbb{H}[U^0] + 4\tau \sum_{n=1}^{L} (\Psi_t^{\alpha,n} U_x, U_x^{n-\theta}) + 4\tau \sum_{n=1}^{L} (Q^{n-\theta}, \Psi_\tau^{\beta,n} Q) + 4\tau \sum_{n=1}^{L} \|U_x^{n-\theta}\|^2 \\ \le&4\tau \left(\sum_{n=1}^{L} (U^{n-\theta}, U_x^{n-\theta}) + \sum_{n=1}^{L} (f(U^{n-\theta}), U_x^{n-\theta}) + \sum_{n=1}^{L} (\hat{g}^{n-\theta}, U^{n-\theta}) \right). \end{aligned} \tag{4.6}$$

By the Hölder inequality and Young inequality, the three terms on the right-hand side of (4.6) can be expanded to

$$\sum_{n=1}^{L} (U^{n-\theta}, U_x^{n-\theta}) \le \frac{1}{2} \sum_{n=1}^{L} \|U^{n-\theta}\|^2 + \frac{1}{2} \sum_{n=1}^{L} \|U_x^{n-\theta}\|^2, \tag{4.7}$$

$$\begin{aligned} \sum_{n=1}^{L} (f(U^{n-\theta}), U_x^{n-\theta}) &\le \sum_{n=1}^{L} \|c_f(U^{n-\theta})\|_\infty \|U^{n-\theta}\| \|U_x^{n-\theta}\| \\ &\le C \sum_{n=1}^{L} \|U^{n-\theta}\|^2 + \frac{1}{2} \sum_{n=1}^{L} \|U_x^{n-\theta}\|^2, \end{aligned} \tag{4.8}$$

$$\sum_{n=1}^{L} (\hat{g}^{n-\theta}, U^{n-\theta}) \le \frac{1}{2} \sum_{n=1}^{L} \|\hat{g}^{n-\theta}\|^2 + \frac{1}{2} \sum_{n=1}^{L} \|U^{n-\theta}\|^2, \tag{4.9}$$

where we use the bounded condition $\|c_f(U^{n-\theta})\|_\infty \le C$.

Substituting (4.7)–(4.9) into (4.6), we arrive at

$$\begin{aligned} &\mathbb{H}[U^L] - \mathbb{H}[U^0] + 4\tau \sum_{n=1}^{L} (\Psi_t^{\alpha,n} U_x, U_x^{n-\theta}) + 4\tau \sum_{n=1}^{L} (Q^{n-\theta}, \Psi_\tau^{\beta,n} Q) \\ \le&C\tau \left(\sum_{n=1}^{L} \|\hat{g}^{n-\theta}\|^2 + \sum_{n=1}^{L} \|U^{n-\theta}\|^2 \right). \end{aligned} \tag{4.10}$$

In what follows, using Lemmas 4.1 and 4.2 and the Gronwall inequality, we have

$$\|U^L\|^2 - \|U^0\|^2 \le C\tau \sum_{n=1}^{L} \|\hat{g}^{n-\theta}\|^2. \tag{4.11}$$

Since $U^0 = 0$, we obtain

$$\|U^L\|^2 \le C\tau \sum_{n=1}^{L} \|\hat{g}^{n-\theta}\|^2. \tag{4.12}$$

Noting that $U^L = u_h^L - \bar{u}_h^0$ and using the triangle inequality, the conclusion of this theorem is derived. □

5. Numerical results

In this section, we present numerical simulation results for both smooth and nonsmooth solutions to verify the effectiveness of the numerical scheme. Next, we set the nonlinear term $f(u) = u^2$, the spatial domain $\Omega = (0, 1)$, and the time interval $J = (0, 1]$.

Example 5.1. The exact solution is $u(x, t) = t^2 \sin(2\pi x)$ satisfying $u(x, 0) = 0$, and the known source function $g(x, t)$ is given by

$$g(x,t) = \sin(2\pi x)\left(2t + \frac{8\pi^2 t^{2-\alpha}}{\Gamma(3-\alpha)} + \frac{32\pi^4 t^{2-\beta}}{\Gamma(3-\beta)} + 4\pi^2 t^2\right) + 2\pi t^2 \cos(2\pi x) + 2\pi t^4 \sin(4\pi x). \tag{5.1}$$

In Table 1, fixing $\tau = 1/1000$ and choosing $h = 1/10, 1/20, 1/40, 1/80$, we provide the L^2-errors and the spatial convergence rates for u and q with different parameters α, β, and θ, where $\theta \le \min\{\alpha, \beta, \frac{1}{2}\}$. Similarly, in Table 2, taking $h = 1/1000$, we calculate the L^2-errors and the time convergence rates with $\tau = 1/10, 1/20, 1/40, 1/80$. From Tables 1 and 2, one can see that the convergence rates in both space and time are close to 2 when the exact solution is smooth. In Table 3, if $\theta > \min\{\alpha, \beta, \frac{1}{2}\}$, the convergence accuracy will be unstable, which verifies the range of θ values from a numerical perspective. To observe the effect of numerical simulation more clearly, we provide the comparison images between numerical solutions and exact solutions. In Figure 1, we show distinct comparison images of the numerical solutions of u_h and q_h and the exact solutions of u and q with $\tau = 1/1000$, $h = 1/80$, $\alpha = 0.2, \beta = 0.8$, and $\theta = 0.2$.

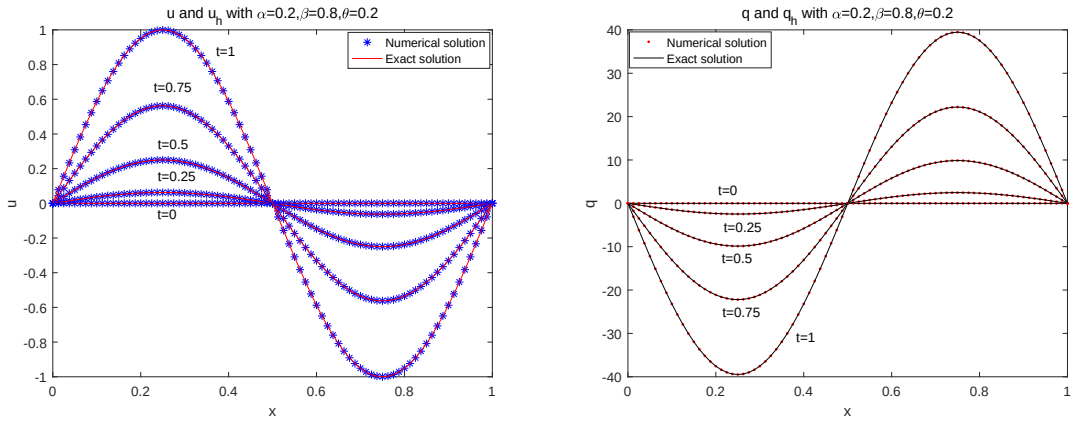

Figure 1. u_h, q_h and u, q with $\tau = 1/1000$, $h = 1/80$, $\alpha = 0.2, \beta = 0.8, \theta = 0.2$

Table 1. Spatial convergence results with $\tau = 1/1000$.

α	β	θ	h	$\|u_h - u\|$	Rate	$\|q_h - q\|$	Rate
			1/10	2.2165E-02	-	2.6449E-02	-
		0.2	1/20	5.6375E-03	1.9752	6.1401E-03	2.1069
			1/40	1.4151E-03	1.9941	1.5121E-03	2.0217
			1/80	3.5399E-04	1.9992	3.8250E-04	1.9830
			1/10	2.2165E-02	-	2.6470E-02	-
0.2	0.8	-0.5	1/20	5.6369E-03	1.9753	6.1607E-03	2.1032
			1/40	1.4146E-03	1.9945	1.5327E-03	2.0070
			1/80	3.5346E-04	2.0008	4.0308E-04	1.9269
			1/10	2.2164E-02	-	2.6490E-02	-
		-1	1/20	5.6364E-03	1.9754	6.1810E-03	2.0996
			1/40	1.4141E-03	1.9949	1.5530E-03	1.9928
			1/80	3.5293E-04	2.0024	4.2346E-04	1.8747
			1/10	2.1828E-02	-	4.0463E-02	-
		0.5	1/20	5.5499E-03	1.9756	9.6844E-03	2.0629
			1/40	1.3932E-03	1.9941	2.3964E-03	2.0148
			1/80	3.4861E-04	1.9987	5.9910E-04	2.0000
			1/10	2.1828E-02	-	4.0465E-02	-
0.5	0.5	0.2	1/20	5.5499E-03	1.9757	9.6868E-03	2.0626
			1/40	1.3931E-03	1.9941	2.3988E-03	2.0137
			1/80	3.4854E-04	1.9989	6.0151E-04	1.9956
			1/10	2.1826E-02	-	4.0523E-02	-
		-1	1/20	5.5484E-03	1.9759	9.7445E-03	2.0561
			1/40	1.3916E-03	1.9953	2.4564E-03	1.9880
			1/80	3.4706E-04	2.0035	6.5921E-04	1.8977
			1/10	2.1399E-02	-	5.8275E-02	-
		0.2	1/20	5.4386E-03	1.9763	1.4195E-02	2.0375
			1/40	1.3651E-03	1.9943	3.5279E-03	2.0085
			1/80	3.4156E-04	1.9988	8.8248E-04	1.9992
			1/10	2.1399E-02	-	5.8276E-02	-
0.8	0.2	0	1/20	5.4386E-03	1.9763	1.4196E-02	2.0374
			1/40	1.3650E-03	1.9943	3.5290E-03	2.0082
			1/80	3.4153E-04	1.9989	8.8360E-04	1.9978
			1/10	2.1396E-02	-	5.8410E-02	-
		-1	1/20	5.4352E-03	1.9769	1.4329E-02	2.0272
			1/40	1.3616E-03	1.9970	3.6619E-03	1.9683
			1/80	3.3812E-04	2.0097	1.0167E-03	1.8487

Table 2. Time convergence results with $h = 1/1000$.

α	β	θ	τ	$\|u_h - u\|$	Rate	$\|q_h - q\|$	Rate
			1/10	1.9614E-03	-	7.7510E-02	-
		0.2	1/20	5.0017E-04	1.9714	1.9814E-02	1.9679
			1/40	1.2703E-04	1.9773	5.0533E-03	1.9712
			1/80	3.2128E-05	1.9832	1.2867E-03	1.9736
			1/10	7.2565E-03	-	2.8650E-01	-
0.2	0.8	-0.5	1/20	1.8309E-03	1.9867	7.2335E-02	1.9858
			1/40	4.6032E-04	1.9919	1.8206E-02	1.9903
			1/80	1.1551E-04	1.9946	4.5778E-03	1.9917
			1/10	1.2197E-02	-	4.8151E-01	-
		-1	1/20	3.1215E-03	1.9662	1.2329E-01	1.9655
			1/40	7.8542E-04	1.9907	3.1091E-02	1.9875
			1/80	1.9579E-04	2.0042	7.8135E-03	1.9924
			1/10	5.3041E-04	-	2.1042E-02	-
		0.5	1/20	1.3386E-04	1.9863	5.3622E-03	1.9724
			1/40	3.3676E-05	1.9910	1.3637E-03	1.9753
			1/80	8.4582E-06	1.9933	3.4761E-04	1.9720
			1/10	1.1457E-03	-	4.5326E-02	-
0.5	0.5	0.2	1/20	2.8884E-04	1.9879	1.1461E-02	1.9836
			1/40	7.2679E-05	1.9907	2.8911E-03	1.9871
			1/80	1.8260E-05	1.9929	7.2972E-04	1.9862
			1/10	1.5622E-02	-	6.1668E-01	-
		-1	1/20	4.0111E-03	1.9615	1.5838E-01	1.9611
			1/40	1.0095E-03	1.9904	3.9868E-02	1.9901
			1/80	2.5362E-04	1.9929	1.0017E-02	1.9928
			1/10	5.2861E-04	-	2.0885E-02	-
		0.5	1/20	1.3465E-04	1.9730	5.3245E-03	1.9717
			1/40	3.4107E-05	1.9811	1.3530E-03	1.9765
			1/80	8.5857E-06	1.9901	3.4270E-04	1.9812
			1/10	2.2763E-03	-	8.9851E-02	-
0.8	0.5	0	1/20	5.7402E-04	1.9875	2.2660E-02	1.9874
			1/40	1.4460E-04	1.9890	5.7086E-03	1.9889
			1/80	3.6405E-05	1.9899	1.4372E-03	1.9898
			1/10	1.5534E-02	-	6.1313E-01	-
		-1	1/20	3.9902E-03	1.9609	1.5749E-01	1.9609
			1/40	1.0033E-03	1.9917	3.9605E-02	1.9916
			1/80	2.5177E-04	1.9946	9.9391E-03	1.9945

Table 3. Time convergence results with $h = 1/1000$.

α	β	θ	τ	$\|u_h - u\|$	Rate	$\|q_h - q\|$	Rate
			1/10	2.4519E-03	-	9.6803E-02	-
0.1	0.9	0.11	1/20	6.2095E-04	1.9813	2.4519E-02	1.9811
			1/40	5.2080E-04	0.2538	2.0647E-02	0.2480
			1/80	4.0699E+02	-19.5758	1.6068E+04	-19.5699
			1/10	1.8093E-03	-	7.1425E-02	-
0.5	0.5	0.51	1/20	4.5109E-04	2.0039	1.7808E-02	2.0039
			1/40	2.0018E-04	1.1721	7.8154E-03	1.1881
			1/80	5.1099E-04	-1.3520	2.0090E-02	-1.3621
			1/10	4.8552E-04	-	1.9119E-02	-
0.8	0.2	0.21	1/20	1.2438E-04	1.9647	4.8398E-03	1.9820
			1/40	5.8298E-05	1.0933	2.2123E-03	1.1294
			1/80	2.3759E-02	-8.6708	9.3790E-01	-8.7277

Example 5.2. In this example, we consider the case where the nonsmooth solution is taken as $u = (t^{\alpha+\beta} + t^3)\sin(2\pi x)$, and the known source term $g(x,t)$ is

$$\begin{aligned} g(x,t) = {} & \sin(2\pi x)\left[(\alpha+\beta)t^{\alpha+\beta-1} + 3t^2 + 4\pi^2\left(\frac{t^\beta\Gamma(\alpha+\beta+1)}{\Gamma(\beta+1)} + \frac{6t^{3-\alpha}}{\Gamma(4-\alpha)}\right)\right] \\ & + \sin(2\pi x)\left[16\pi^4\left(\frac{t^\alpha\Gamma(\alpha+\beta+1)}{\Gamma(\alpha+1)} + \frac{6t^{3-\beta}}{\Gamma(4-\beta)}\right) + 4\pi^2(t^{\alpha+\beta} + t^3)\right] \\ & + 2\pi(t^{\alpha+\beta} + t^3)\cos(2\pi x) + 2\pi(t^{\alpha+\beta} + t^3)^2\sin(4\pi x). \end{aligned} \tag{5.2}$$

Table 4 presents the L^2-errors and the spatial convergence rates of u and q before and after adding the starting parts with $h = 1/10, 1/20, 1/40, 1/80$, $\tau = 1/2000$, where Error_o denotes the error before adding the starting parts and Error_c denotes the error after adding the starting parts.

Table 4. Spatial convergence results with $\alpha = 0.9, \beta = 0.2, \tau = 1/2000$.

		$\|u_h - u\|$				$\|q_h - q\|$			
θ	h	Error_o	Rate	Error_c	Rate	Error_o	Rate	Error_c	Rate
	1/10	4.2694E-02	-	4.2693E-02	-	1.2162E-01	-	1.2163E-01	-
0.2	1/20	1.0850E-02	1.9763	1.0850E-02	1.9763	2.9675E-02	2.0351	2.9679E-02	2.0349
	1/40	2.7235E-03	1.9942	2.7234E-03	1.9942	7.3708E-03	2.0094	7.3746E-03	2.0088
	1/80	6.8165E-04	1.9984	6.8155E-04	1.9985	1.8361E-03	2.0051	1.8400E-03	2.0029
	1/10	4.2693E-02	-	4.2692E-02	-	1.2165E-01	-	1.2168E-01	-
-0.5	1/20	1.0849E-02	1.9764	1.0849E-02	1.9764	2.9706E-02	2.0340	2.9728E-02	2.0331
	1/40	2.7227E-03	1.9945	2.7221E-03	1.9947	7.4017E-03	2.0048	7.4237E-03	2.0016
	1/80	6.8085E-04	1.9996	6.8028E-04	2.0005	1.8671E-03	1.9871	1.8891E-03	1.9744
	1/10	4.2691E-02	-	4.2690E-02	-	1.2172E-01	-	1.2177E-01	-
-1	1/20	1.0848E-02	1.9766	1.0846E-02	1.9767	2.9776E-02	2.0314	2.9822E-02	2.0297
	1/40	2.7209E-03	1.9952	2.7197E-03	1.9957	7.4714E-03	1.9947	7.5178E-03	1.9880
	1/80	6.7905E-04	2.0025	6.7786E-04	2.0044	1.9368E-03	1.9477	1.9833E-03	1.9224

The spatial convergence rate is almost unaffected before and after correction, based on a comparison of the data in Table 5. In Tables 6 and 7, we present the L^2-errors and the time convergence rates of u and q before and after adding the starting parts. Without the addition of the starting parts, the time convergence rates are unstable and cannot reach the second-order convergence results computed by the generalized BDF2-θ. After adding the starting parts, the time convergence rates keep around 2, indicating that the starting part plays a major role in correcting the time convergence rates.

Table 5. Spatial convergence results with $\alpha = 0.5, \beta = 0.7, \tau = 1/2000$.

		$\|u_h - u\|$				$\|q_h - q\|$			
θ	h	Error_o	Rate	Error_c	Rate	Error_o	Rate	Error_c	Rate
	1/10	4.3949E-02	-	4.3948E-02	-	6.8838E-02	-	6.8891E-02	-
0.5	1/20	1.1177E-02	1.9753	1.1176E-02	1.9754	1.6266E-02	2.0814	1.6318E-02	2.0778
	1/40	2.8070E-03	1.9934	2.8057E-03	1.9940	3.9696E-03	2.0348	4.0219E-03	2.0205
	1/80	7.0358E-04	1.9963	7.0222E-04	1.9984	9.4708E-04	2.0674	9.9935E-04	2.0088
	1/10	4.3949E-02	-	4.3948E-02	-	6.8842E-02	-	6.8897E-02	-
0.2	1/20	1.1177E-02	1.9753	1.1176E-02	1.9754	1.6270E-02	2.0811	1.6324E-02	2.0774
	1/40	2.8069E-03	1.9935	2.8055E-03	1.9940	3.9739E-03	2.0336	4.0279E-03	2.0189
	1/80	7.0346E-04	1.9964	7.0206E-04	1.9986	9.5140E-04	2.0624	1.0054E-03	2.0023
	1/10	4.3948E-02	-	4.3946E-02	-	6.8877E-02	-	6.8974E-02	-
-1	1/20	1.1176E-02	1.9754	1.1174E-02	1.9756	1.6304E-02	2.0788	1.6401E-02	2.0722
	1/40	2.8061E-03	1.9938	2.8035E-03	1.9948	4.0077E-03	2.0244	4.1049E-03	1.9984
	1/80	7.0259E-04	1.9978	7.0007E-04	2.0017	9.8520E-04	2.0243	1.0824E-03	1.9231

Table 6. Time convergence results with $\alpha = 0.9, \beta = 0.2, h = 1/2000$.

		$\|u_h - u\|$				$\|q_h - q\|$			
θ	τ	Error_o	Rate	Error_c	Rate	Error_o	Rate	Error_c	Rate
	1/10	2.1916E-03	-	4.2694E-02	-	8.6515E-02	-	1.2162E-01	-
0.2	1/20	1.6194E-03	0.4365	1.0850E-02	1.9763	6.3929E-02	0.4365	2.9675E-02	2.0351
	1/40	1.0890E-03	0.5725	2.7235E-03	1.9942	4.2990E-02	0.5725	7.3710E-03	2.0093
	1/80	6.8790E-04	0.6627	6.8165E-04	1.9984	2.7157E-02	0.6627	1.8364E-03	2.0050
	1/10	2.5540E-03	-	4.2693E-02	-	1.0123E-01	-	1.2164E-01	-
0	1/20	1.1111E-03	1.2007	1.0850E-02	1.9763	4.3864E-02	1.2065	2.9692E-02	2.0345
	1/40	7.7616E-04	0.5176	2.7231E-03	1.9944	3.0641E-02	0.5176	7.3878E-03	2.0069
	1/80	5.0234E-04	0.6277	6.8122E-04	1.9990	1.9831E-02	0.6277	1.8531E-03	1.9952
	1/10	2.4652E-02	-	4.2689E-02	-	9.7312E-01	-	1.2182E-01	-
-0.5	1/20	7.1878E-03	1.7781	1.0845E-02	1.9768	2.8376E-01	1.7779	2.9872E-02	2.0279
	1/40	1.9420E-03	1.8880	2.7184E-03	1.9962	7.6702E-02	1.8874	7.5673E-03	1.9809
	1/80	5.5906E-04	1.7965	6.7658E-04	2.0064	2.2071E-02	1.7971	2.0329E-03	1.8962

Table 7. Time convergence results with $\alpha = 0.5$, $\beta = 0.7$, $h = 1/2000$.

		$\|u_h - u\|$				$\|q_h - q\|$			
θ	τ	Error_o	Rate	Error_c	Rate	Error_o	Rate	Error_c	Rate
	1/10	1.1456E-02	-	4.3948E-02	-	4.5228E-01	-	6.8880E-02	-
0.5	1/20	5.0680E-03	1.1767	1.1176E-02	1.9754	2.0008E-01	1.1767	1.6307E-02	2.0786
	1/40	2.2184E-03	1.1919	2.8060E-03	1.9939	8.7577E-02	1.1919	4.0110E-03	2.0235
	1/80	9.6796E-04	1.1965	7.0250E-04	1.9979	3.8213E-02	1.1965	9.8850E-04	2.0207
	1/10	5.4375E-03	-	4.3948E-02	-	2.1466E-01	-	6.8904E-02	-
0.2	1/20	2.5220E-03	1.1084	1.1176E-02	1.9754	9.9562E-02	1.1084	1.6332E-02	2.0769
	1/40	1.1387E-03	1.1472	2.8053E-03	1.9941	4.4952E-02	1.1472	4.0351E-03	2.0170
	1/80	5.0160E-04	1.1828	7.0188E-04	1.9989	1.9802E-02	1.1827	1.0126E-03	1.9946
	1/10	2.8636E-02	-	4.3948E-02	-	1.1304E+00	-	6.8904E-02	-
-1	1/20	7.7097E-03	1.8931	1.1176E-02	1.9754	3.0439E-01	1.8929	1.6332E-02	2.0769
	1/40	1.9098E-03	2.0133	2.8053E-03	1.9941	7.5437E-02	2.0126	4.0351E-03	2.0170
	1/80	6.3574E-04	1.5869	7.0188E-04	1.9989	2.5098E-02	1.5877	1.0126E-03	1.9946

In Figure 2, we obtain the comparison images between the numerical solution and the exact solution with $\tau = 1/1000$, $h = 1/80$, $\alpha = 0.9$, $\beta = 0.2$, and $\theta = 0.2$. In Figures 3 and 4, we present the space and time convergence rate images of u_h and q_h under different parameters α, β, and θ. From Figure 4, one can see that the corrected scheme with the starting parts can effectively restore the second-order convergence rate for the nonsmooth problem.

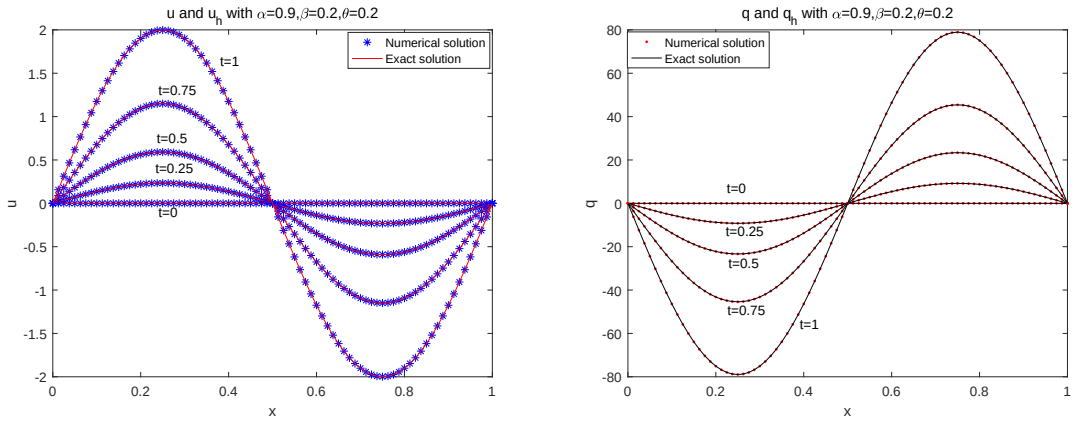

Figure 2. u_h, q_h and u, q with $\tau = 1/2000$, $h = 1/80$, $\alpha = 0.9$, $\beta = 0.2$, $\theta = 0.2$.

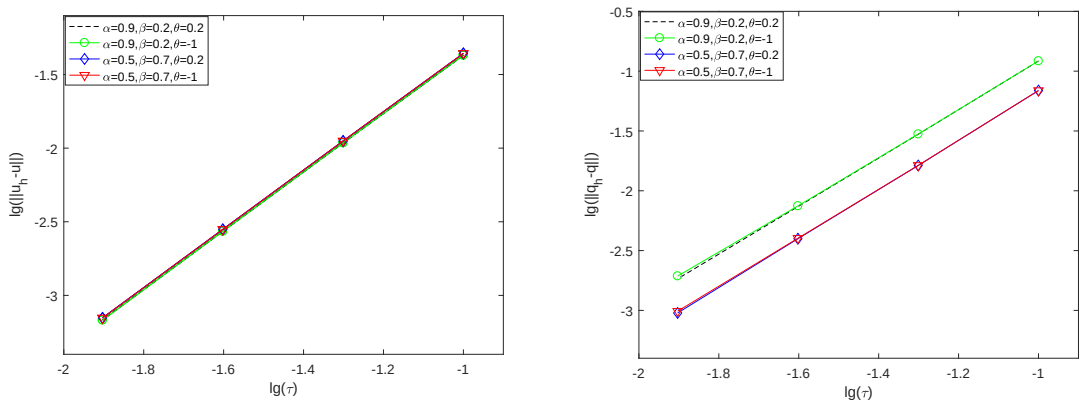

Figure 3. The spatial convergence rates in L^2-errors with different parameters α, β, and θ.

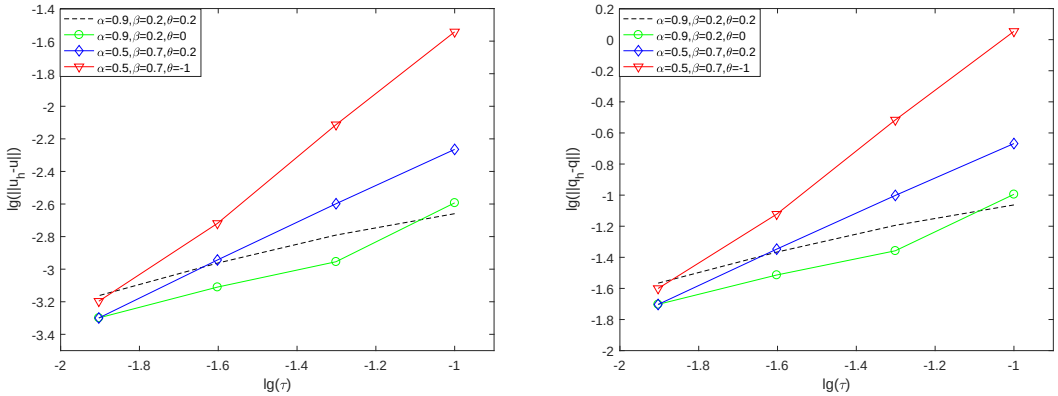

(a) The time convergence rates of $\|u - u_h\|$ and $\|q - q_h\|$ without starting parts

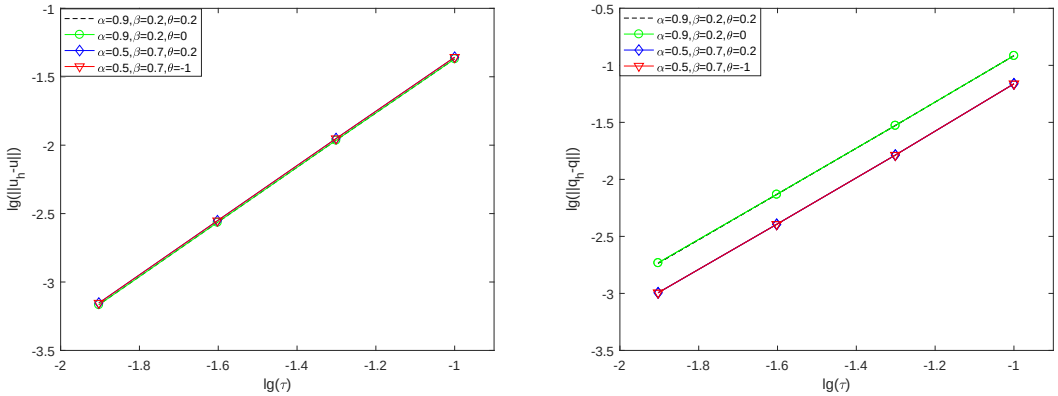

(b) The time convergence rates of $\|u - u_h\|$ and $\|q - q_h\|$ with starting parts

Figure 4. The time convergence rates in L^2-errors with different parameters α, β, and θ.

Example 5.3. To better investigate the effect of changes of two fractional parameters α and β on the convergence rates, we introduce the numerical example with two nonsmooth terms. Here, we take the nonsmooth solution u with

$$u = (t^{1+\alpha} + t^{1+\beta} + t^3)\sin(2\pi x),$$

and the known source term

$$\begin{aligned} g(x,t) = {} & \sin(2\pi x)\left[(1+\alpha)t^{\alpha} + (1+\beta)t^{\beta} + 3t^2 + 4\pi^2\left(t\Gamma(2+\alpha) + \frac{t^{1+\beta-\alpha}\Gamma(2+\beta)}{\Gamma(2+\beta-\alpha)} + \frac{6t^{3-\alpha}}{\Gamma(4-\alpha)}\right)\right] \\ & + \sin(2\pi x)\left[16\pi^4\left(\frac{t^{1+\alpha-\beta}\Gamma(2+\alpha)}{\Gamma(2+\alpha-\beta)} + t\Gamma(2+\beta) + \frac{6t^{3-\beta}}{\Gamma(4-\beta)}\right) + 4\pi^2(t^{1+\alpha} + t^{1+\beta} + t^3)\right] \\ & + 2\pi(t^{1+\alpha} + t^{1+\beta} + t^3)\cos(2\pi x) + 2\pi(t^{1+\alpha} + t^{1+\beta} + t^3)^2\sin(4\pi x). \end{aligned} \tag{5.3}$$

In Table 8, we provide the errors of $\|u_h - u\|$ and $\|q_h - q\|$ and the spatial convergence rates under different parameters, which indicate that the corrected term hardly affects the spatial convergence rate.

In Tables 9–11, fixing $\tau = 1/4000$, choosing $h = 1/10, 1/20, 1/40, 1/80$, and changing parameters α, β, and θ, we provide the L^2-errors and the time convergence rates for u and q based on the corrected scheme and uncorrected scheme. The impact of different fractional parameters on the time convergence rates of nonsmooth problems is evident from Tables 9–11. Furthermore, one can see that the corrected scheme with the starting part can effectively restore the second-order convergence rate.

To further validate the performance of the parameter θ in numerical simulations with nonsmooth solutions, we provide the computing data in Table 12, from which one can see that the parameter θ still needs to satisfy $\theta \le \min\{\alpha, \beta, \frac{1}{2}\}$, whether before or after correction. Notably, when θ is negative, as long as it is not much less than 0, we can still obtain second-order convergence accuracy.

Table 8. Spatial convergence results with $\alpha = 0.5, \beta = 0.6, \tau = 1/2000$.

		$\|u_h - u\|$				$\|q_h - q\|$			
θ	h	Error$_o$	Rate	Error$_c$	Rate	Error$_o$	Rate	Error$_c$	Rate
	1/10	6.5710E-02	-	6.5710E-02	-	1.1335E-01	-	1.1335E-01	-
0.5	1/20	1.6709E-02	1.9755	1.6709E-02	1.9755	2.7037E-02	2.0678	2.7037E-02	2.0678
	1/40	4.1946E-03	1.9940	4.1946E-03	1.9940	6.6773E-03	2.0176	6.6775E-03	2.0175
	1/80	1.0498E-03	1.9984	1.0498E-03	1.9984	1.6615E-03	2.0068	1.6617E-03	2.0066
	1/10	6.5710E-02	-	6.5710E-02	-	1.1336E-01	-	1.1336E-01	-
0.2	1/20	1.6708E-02	1.9755	1.6708E-02	1.9755	2.7042E-02	2.0676	2.7042E-02	2.0676
	1/40	4.1944E-03	1.9940	4.1944E-03	1.9940	6.6826E-03	2.0167	6.6825E-03	2.0167
	1/80	1.0497E-03	1.9986	1.0497E-03	1.9985	1.6668E-03	2.0033	1.6667E-03	2.0034
	1/10	6.5709E-02	-	6.5709E-02	-	1.1339E-01	-	1.1339E-01	-
-0.5	1/20	1.6708E-02	1.9756	1.6708E-02	1.9756	2.7078E-02	2.0661	2.7077E-02	2.0662
	1/40	4.1935E-03	1.9943	4.1935E-03	1.9943	6.7188E-03	2.0109	6.7178E-03	2.0110
	1/80	1.0487E-03	1.9995	1.0487E-03	1.9995	1.7031E-03	1.9801	1.7020E-03	1.9808

Table 9. Time convergence results with $\alpha = 0.1, \beta = 0.9, h = 1/4000$.

		$\|u_h - u\|$				$\|q_h - q\|$			
θ	τ	Error_o	Rate	Error_c	Rate	Error_o	Rate	Error_c	Rate
	1/10	8.9204E-03	-	6.2820E-03	-	3.5216E-01	-	2.4809E-01	-
0.1	1/20	5.2261E-03	0.7714	1.8535E-03	1.7609	2.0632E-01	0.7714	7.3209E-02	1.7608
	1/40	2.6562E-03	0.9764	4.9663E-04	1.9001	1.0486E-01	0.9764	1.9628E-02	1.8992
	1/80	1.2855E-03	1.0470	1.2782E-04	1.9580	5.0749E-02	1.0470	5.0645E-03	1.9544
	1/10	1.1291E-02	-	9.1163E-03	-	4.4575E-01	-	3.5998E-01	
0	1/20	6.8182E-03	0.7277	2.7085E-03	1.7510	2.6917E-01	0.7277	1.0696E-01	1.7509
	1/40	3.4949E-03	0.9641	7.2773E-04	1.8960	1.3797E-01	0.9641	2.8751E-02	1.8954
	1/80	1.6987E-03	1.0408	1.8766E-04	1.9553	6.7062E-02	1.0408	7.4268E-03	1.9528
	1/10	2.1457E-02	-	2.6030E-02	-	1.1105E+00	-	1.7696E+00	-
-0.5	1/20	1.4552E-02	0.5603	8.3150E-03	1.6464	8.5207E-01	0.3822	6.2053E-01	1.5118
	1/40	7.7887E-03	0.9017	2.2980E-03	1.8554	4.7736E-01	0.8359	1.7762E-01	1.8047
	1/80	3.8350E-03	1.0222	6.0067E-04	1.9357	2.3888E-01	0.9988	4.7205E-02	1.9118

Table 10. Time convergence results with $\alpha = 0.5, \beta = 0.6, h = 1/4000$

		$\|u_h - u\|$				$\|q_h - q\|$			
θ	τ	Error_o	Rate	Error_c	Rate	Error_o	Rate	Error_c	Rate
	1/10	4.3621E-03	-	3.6704E-03	-	1.7226E-01	-	1.4498E-01	-
0.5	1/20	1.0876E-03	2.0039	9.5152E-04	1.9476	4.2941E-02	2.0042	3.7576E-02	1.9480
	1/40	3.3133E-04	1.7148	2.4178E-04	1.9765	1.3080E-02	1.7150	9.5356E-03	1.9784
	1/80	1.1132E-04	1.5735	6.1138E-05	1.9835	4.3948E-03	1.5735	2.3985E-03	1.9912
	1/10	1.4643E-03	-	1.0614E-03	-	5.8318E-02	-	4.2803E-02	-
0.2	1/20	4.8956E-04	1.5806	3.0032E-04	1.8214	1.9326E-02	1.5934	1.2126E-02	1.8197
	1/40	1.6670E-04	1.5542	7.8625E-05	1.9335	6.5811E-03	1.5541	3.1895E-03	1.9267
	1/80	5.7051E-05	1.5470	1.9768E-05	1.9918	2.2523E-03	1.5470	8.1546E-04	1.9676
	1/10	8.7609E-03	-	6.8360E-03	-	3.4601E-01	-	2.7011E-01	-
0	1/20	2.2404E-03	1.9673	1.9129E-03	1.8374	8.8510E-02	1.9669	7.5599E-02	1.8371
	1/40	5.6418E-04	1.9895	5.0061E-04	1.9340	2.2304E-02	1.9886	1.9798E-02	1.9330
	1/80	1.5985E-04	1.8194	1.2738E-04	1.9746	6.3107E-03	1.8214	5.0505E-03	1.9709

Table 11. Time convergence results with $\alpha = 0.9, \beta = 0.1, h = 1/4000$

		$\|u_h - u\|$				$\|q_h - q\|$			
θ	τ	Error_o	Rate	Error_c	Rate	Error_o	Rate	Error_c	Rate
	1/10	1.2779E-03	-	4.4043E-04	-	5.0452E-02	-	2.5629E-02	-
0.1	1/20	1.0267E-03	0.3157	1.1804E-04	1.8996	4.0534E-02	0.3158	7.0942E-03	1.8531
	1/40	7.5884E-04	0.4362	3.0793E-05	1.9386	2.9957E-02	0.4362	1.8662E-03	1.9265
	1/80	5.0089E-04	0.5993	8.1141E-06	1.9241	1.9774E-02	0.5993	4.7828E-04	1.9642
	1/10	4.3621E-03	-	1.4545E-03	-	7.7482E-02	-	6.1261E-02	-
0	1/20	1.8873E-03	0.6822	3.9496E-04	1.8807	4.6434E-02	0.7387	1.6763E-02	1.8697
	1/40	9.2034E-04	0.3539	1.0228E-04	1.9492	3.6333E-02	0.3539	4.3730E-03	1.9386
	1/80	6.1337E-04	0.5854	2.5740E-05	1.9904	2.4215E-02	0.5854	1.1169E-03	1.9692
	1/10	9.0746E-03	-	6.1035E-03	-	3.5896E-01	-	2.4209E-01	-
-0.1	1/20	2.3761E-03	1.9332	1.7550E-03	1.7982	9.4044E-02	1.9324	6.9621E-02	1.7980
	1/40	7.1647E-04	1.7296	4.6664E-04	1.9111	2.8284E-02	1.7333	1.8526E-02	1.9100
	1/80	5.9682E-04	0.2636	1.1984E-04	1.9612	2.3561E-02	0.2636	4.7711E-03	1.9572

Table 12. Time convergence results with $\alpha = 0.7, \beta = 0.3, h = 1/4000$

		$\|u_h - u\|$				$\|q_h - q\|$			
θ	τ	Error_o	Rate	Error_c	Rate	Error_o	Rate	Error_c	Rate
	1/10	3.3675E-03	-	2.0604E-03	-	1.3333E-01	-	8.2027E-02	-
0.31	1/20	1.2977E-03	1.3757	5.3018E-04	1.9584	5.1287E-02	1.3783	2.1127E-02	1.9570
	1/40	1.9442E-03	-0.5833	1.4145E-04	1.9062	7.6738E-02	-0.5813	5.6232E-03	1.9096
	1/80	6.1733E-02	-4.9888	1.3510E-04	0.0663	2.4372E+00	-4.9892	5.3212E-03	0.0797
	1/10	4.5472E-02	-	3.0346E-02	-	1.7952E+00	-	1.1983E+00	-
-0.5	1/20	1.2127E-02	1.9067	9.1861E-03	1.7240	4.7880E-01	1.9066	3.6273E-01	1.7240
	1/40	3.1344E-03	1.9520	2.4851E-03	1.8861	1.2376E-01	1.9518	9.8141E-02	1.8859
	1/80	7.9608E-04	1.9772	6.4304E-04	1.9504	3.1447E-02	1.9766	2.5407E-02	1.9496
	1/10	1.1762E+00	-	3.4223E-01	-	4.6430E+01	-	1.3512E+01	-
-5	1/20	3.9521E-01	1.5734	1.9704E-01	0.7964	1.5601E+01	1.5734	7.7788E+00	0.7966
	1/40	1.2069E-01	1.7113	7.7857E-02	1.3396	4.7643E+00	1.7113	3.0736E+00	1.3396
	1/80	3.3458E-02	1.8509	2.4673E-02	1.6579	1.3208E+00	1.8509	9.7402E-01	1.6579

The time convergence rates of u and q are compared before and after correction with different parameters α, β, and θ in Figure 5, where the slope of the line segment indicates the convergence rate. The slope of each line segment in the corrected images is the same regardless of the parameters chosen, indicating that the introduction of the starting part has a significant effect on the time convergence rates for the case with nonsmooth solutions.

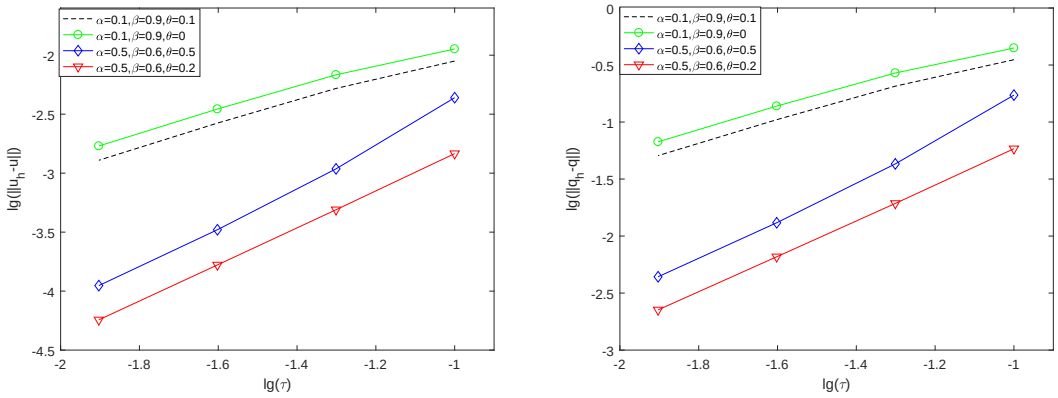

(a) The time convergence rates of $\|u - u_h\|$ and $\|q - q_h\|$ without starting parts

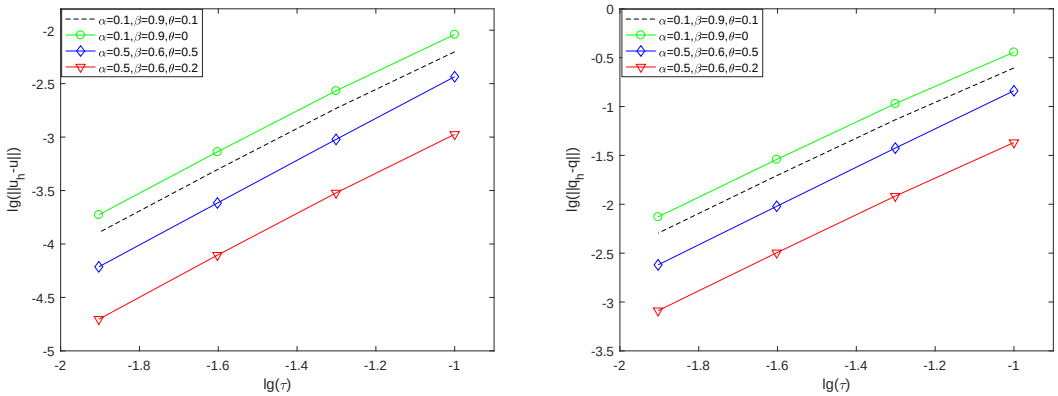

(b) The time convergence rates of $\|u - u_h\|$ and $\|q - q_h\|$ with starting parts

Figure 5. The time convergence rates in L^2-errors with different parameters α, β, and θ.

6. Conclusions

In this article, the spatial mixed finite element method with the generalized BDF2-θ for solving the time-fractional generalized Rosenau-RLW-Burgers equation was presented. Detailed proofs of stability were shown. The numerical scheme's effectiveness and feasibility were verified by conducting numerical examples that included both smooth and nonsmooth solutions. The numerical examples with good regularity indicated that our algorithm with changed parameters α, β, and θ can maintain second-order convergence in time. Especially, the nonsmooth examples demonstrated that adding the correction term could effectively solve the problem of reduced order caused by weak singularity.

Author contributions

N. Yang: Writing–original draft, Formal analysis, Software; Y. Liu: Methodology, Validation, Formal analysis, Funding acquisition, Supervision, Writing–review & editing. All authors have read and agreed to the published version of the manuscript.

Use of Generative-AI tools declaration

The authors declare they have not used Artificial Intelligence (AI) tools in the creation of this article.

Acknowledgments

This work was supported by the National Natural Science Foundation of China (12061053), Young Innovative Talents Project of Grassland Talents Project and Program for Innovative Research Team in Universities of Inner Mongolia Autonomous Region (NMGIRT2413).

Conflict of interest

The authors declare that they have no conflicts of interest.

References

1. N. Atouani, K. Omrani, Galerkin finite element method for the Rosenau-RLW equation, *Comput. Math. Appl.*, **66** (2013), 289–303. https://doi.org/10.1016/j.camwa.2013.04.029
2. D. D. He, K. J. Pan, A linearly implicit conservative difference scheme for the generalized Rosenau-Kawahara-RLW equation, *Appl. Math. Comput.*, **271** (2015), 323–336. https://doi.org/10.1016/j.amc.2015.09.021
3. B. Wongsaijai, K. Poochinapan, Optimal decay rates of the dissipative shallow water waves modeled by coupling the Rosenau-RLW equation and the Rosenau-Burgers equation with power of nonlinearity, *Appl. Math. Comput.*, **405** (2021), 126202. https://doi.org/10.1016/j.amc.2021.126202
4. T. Mouktonglang, S. Yimnet, N. Sukantamala, B. Wongsaijai, Dynamical behaviors of the solution to a periodic initial-boundary value problem of the generalized Rosenau-RLW-Burgers equation, *Math. Comput. Simul.*, **196** (2022), 114–136. https://doi.org/10.1016/j.matcom.2022.01.004
5. X. F. Wang, W. Z. Dai, A new implicit energy conservative difference scheme with fourth-order accuracy for the generalized Rosenau-Kawahara-RLW equation, *Comput. Appl. Math.*, **37** (2018), 6560–6581. https://doi.org/10.1007/s40314-018-0685-4
6. S. F. Alrzqi, F. A. Alrawajeh, H. N. Hassan, An efficient numerical technique for investigating the generalized Rosenau-KdV-RLW equation by using the Fourier spectral method, *AIMS Math.*, **9** (2024), 8661–8688. https://doi.org/10.3934/math.2024420
7. M. Mustahsan, A. Kiran, J. Singh, K. S. Nisar, D. Kumar, Higher order B-spline differential quadrature rule to approximate generalized Rosenau-RLW equation, *Math. Methods Appl. Sci.*, **43** (2020), 6812–6822. https://doi.org/10.1002/mma.6423
8. Y. Shi, X. H. Yang, Z. M. Zhang, Construction of a new time-space two-grid method and its solution for the generalized Burgers' equation, *Appl. Math. Lett.*, **158** (2024), 109244. https://doi.org/10.1016/j.aml.2024.109244
9. G. R. Piao, F. Yao, W. Zhao, Reduced basis finite element methods for the Korteweg-de Vries-Burgers equation, *Int. J. Numer. Anal. Model.*, **19** (2022), 369–385.

10. X. H. Yang, W. L. Qiu, H. F. Chen, H. X. Zhang, Second-order BDF ADI Galerkin finite element method for the evolutionary equation with a nonlocal term in three-dimensional space, *Appl. Numer. Math.*, **172** (2022), 497–513. https://doi.org/10.1016/j.apnum.2021.11.004
11. M. Kamiński, M. Guminiak, A. Lenartowicz, M. Łasecka-Plura, M. Przychodzki, W. Sumelka, Eigenvibrations of Kirchhoff rectangular random plates on time-fractional viscoelastic supports via the stochastic finite element method, *Materials*, **16** (2023), 1–32. https://doi.org/10.3390/ma16247527
12. Y. Liu, Y. W. Du, H. Li, F. W. Liu, Y. J. Wang, Some second-order θ schemes combined with finite element method for nonlinear fractional cable equation, *Numer. Algor.*, **80** (2019), 533–555. https://doi.org/10.1007/s11075-018-0496-0
13. D. F. Li, C. J. Zhang, M. H. Ran, A linear finite difference scheme for generalized time fractional Burgers equation, *Appl. Math. Model.*, **40** (2016), 6069–6081. https://doi.org/10.1016/j.apm.2016.01.043
14. H. Sun, Z. Z. Sun, G. H. Gao, Some temporal second order difference schemes for fractional wave equations, *Numer. Methods Partial Differ. Equ.*, **32** (2016), 970–1001. https://doi.org/10.1002/num.22038
15. G. H. Gao, H. W. Sun, Z. Z. Sun, Stability and convergence of finite difference schemes for a class of time fractional sub-diffusion equations based on certain superconvergence, *J. Comput. Phys.*, **280** (2015), 510–528. https://doi.org/10.1016/j.jcp.2014.09.033
16. L. B. Feng, P. Zhuang, F. Liu, I. Turner, Stability and convergence of a new finite volume method for a two-sided space-fractional diffusion equation, *Appl. Math. Comput.*, **257** (2015), 52–65. https://doi.org/10.1016/j.amc.2014.12.060
17. A. Cardone, R. D'Ambrosio, B. Paternoster, A spectral method for stochastic fractional differential equations, *Appl. Numer. Math.*, **139** (2019), 115–119. https://doi.org/10.1016/j.apnum.2019.01.009
18. L. Chen, S. J. Lü, T. Xu, Fourier spectral approximation for time fractional Burgers equation with nonsmooth solutions, *Appl. Numer. Math.*, **169** (2021), 164–178. https://doi.org/10.1016/j.apnum.2021.05.022
19. M. Hussain, S. Haq, A. Ghafoor, I. Ali, Numerical solutions of time-fractional coupled viscous Burgers' equations using meshfree spectral method, *Comput. Appl. Math.*, **39** (2020), 6. https://doi.org/10.1007/s40314-019-0985-3
20. X. F. Liu, X. Y. Yang, Mixed finite element method for the nonlinear time-fractional stochastic fourth-order reaction-diffusion equation, *Comput. Math. Appl.*, **84** (2021), 39–55. https://doi.org/10.1016/j.camwa.2020.12.004
21. C. Wen, Y. Liu, B. L. Yin, H. Li, J. F. Wang, Fast second-order time two-mesh mixed finite element method for a nonlinear distributed-order sub-diffusion model, *Numer. Algor.*, **88** (2021), 523–553. https://doi.org/10.1007/s11075-020-01048-8
22. Y. Wang, Y. N. Yang, J. F. Wang, H. Li, Y. Liu, Unconditional analysis of the linearized second-order time-stepping scheme combined with a mixed element method for a nonlinear time fractional fourth-order wave equation, *Comput. Math. Appl.*, **157** (2024), 74–91. https://doi.org/10.1016/j.camwa.2023.12.023

23. C. Lubich, Discretized fractional calculus, *SIAM J. Math. Anal.*, **17** (1986), 704–719. https://doi.org/10.1137/0517050
24. H. B. Chen, D. Xu, Y. L. Peng, An alternating direction implicit fractional trapezoidal rule type difference scheme for the two-dimensional fractional evolution equation, *Int. J. Comput. Math.*, **92** (2015), 2178–2197. https://doi.org/10.1080/00207160.2014.975694
25. B. T. Jin, B. Y. Li, Z. Zhou, Correction of high-order BDF convolution quadrature for fractional evolution equations, *SIAM J. Sci. Comput.*, **39** (2017), A3129–A3152. https://doi.org/10.1137/17M1118816
26. Y. Liu, B. L. Yin, H. Li, Z. M. Zhang, The unified theory of shifted convolution quadrature for fractional calculus, *J. Sci. Comput.*, **89** (2021), 18. https://doi.org/10.1007/s10915-021-01630-9
27. B. L. Yin, Y. Liu, H. Li, A class of shifted high-order numerical methods for the fractional mobile/immobile transport equations, *Appl. Math. Comput.*, **368** (2020), 124799. https://doi.org/10.1016/j.amc.2019.124799
28. Y. X. Niu, J. F. Wang, Y. Liu, H. Li, Z. C. Fang, Local discontinuous Galerkin method based on a family of second-order time approximation schemes for fractional mobile/immobile convection-diffusion equations, *Appl. Numer. Math.*, **179** (2022), 149–169. https://doi.org/10.1016/j.apnum.2022.04.020
29. B. T. Jin, R. Lazarov, Z. Zhou, Two fully discrete schemes for fractional diffusion and diffusion-wave equations with nonsmooth data, *SIAM J. Sci. Comput.*, **38** (2016), A146–A170. https://doi.org/10.1137/140979563
30. F. H. Zeng, C. P. Li, F. W. Liu, I. Turner, Numerical algorithms for time-fractional subdiffusion equation with second-order accuracy, *SIAM J. Sci. Comput.*, **37** (2015), A55–A78. https://doi.org/10.1137/14096390X
31. L. Galeone, R. Garrappa, Explicit methods for fractional differential equations and their stability properties, *J. Comput. Appl. Math.*, **228** (2009), 548–560. https://doi.org/10.1016/j.cam.2008.03.025
32. F. H. Zeng, I. Turner, K. Burrage, G. E. Karniadakis, A new class of semi-implicit methods with linear complexity for nonlinear fractional differential equations, *SIAM J. Sci. Comput.*, **40** (2018), A2986–A3011. https://doi.org/10.1137/18M1168169
33. L. Chai, Y. Liu, H. Li, Fourth-order compact difference schemes for the two-dimensional nonlinear fractional mobile/immobile transport models, *Comput. Math. Appl.*, **100** (2021), 1–10. https://doi.org/10.1016/j.camwa.2021.08.027
34. N. Atouani, Y. Ouali, K. Omrani, Mixed finite element methods for the Rosenau equation, *J. Appl. Math. Comput.*, **57** (2018), 393–420. https://doi.org/10.1007/s12190-017-1112-5
35. A. K. Pani, An H^1-Galerkin mixed finite element method for parabolic partial differential equations, *SIAM J. Numer. Anal.*, **35** (1998), 712–727. https://doi.org/10.1137/S0036142995280808
36. T. H. Robey, The primal mixed finite element method and the LBB condition, *Numer. Methods Partial Differ. Equ.*, **8** (1992), 357–379. https://doi.org/10.1002/num.1690080405

AIMS Press